Inorganic Nanotubes

DOI: 10.1002/ange.200601024

Hollow and Tin-Filled Nanotubes of Single-Crystalline $In(OH)_3$ Grown by a Solution–Liquid–Solid–Solid Route**

*Yueping Fang, Xiaogang Wen, and Shihe Yang**

A variety of methods have been employed in recent years to produce nanowires and nanorods of metals/semiconductors with heterostructures such as coaxial core–shell[1] and composite[2] nanostructures, which appear promising for the nanoscale manipulation of particles/quasi-particles such as electrons and photons. However, these methods often involve tedious procedures, harsh conditions, or expensive instrumentation. For example, multi-step depositions involving sequential charging of desired source materials[3] or surface modification by ambient species[4] are necessary for the preparation of coaxial core–shell nanowires. Herein, we demonstrate an extension of the solution–liquid–solid (SLS) method for the first synthesis of Sn-filled $In(OH)_3$ nanotubes in what is essentially a one-step solution–liquid–solid–solid (SLSS) growth process.

The solution–liquid–solid (SLS) growth of nanowires was first reported by Buhro and co-workers, who used nanoparticles of a low melting point metal (e.g., In and Ga, etc.) in an organic solution to induce the growth of GaAs nanowires with a narrow diameter distribution.[5] In a related work, Korgel et al. successfully synthesized carbon nanotubes and defect-free Si nanowires by SLS growth in supercritical fluids.[6] However, the SLS method has not been used for the growth of inorganic nanotubes up till now. We are able to assemble Sn-filled $In(OH)_3$ nanotubes using liquid droplets of an In–Sn mixture, which serves as both catalyst and reagents for the nanotube growth, from an ethanol-containing aqueous solution under an oxidative atmosphere.

Indium hydroxide is a rather interesting material due to its special semiconducting and optical properties. Ishida and Kuwabara,[7] for example, have shown that the conductivity of $In(OH)_3$ thin-films varies from 10^{-7} to $10^{-3}\,S\,cm^{-2}$ depending on the experimental conditions, which is typical for a wide-bandgap semiconductor, and the optical bandgap, E_g, of needle-like nanoparticles of indium hydroxide has been estimated to be 5.15 eV by diffuse reflectance spectroscopy (DRS) using the Kubelka–Munk (KM) technique.[8] Although nanowires of $In(OH)_3$ have been reported recently,[9] currently available approaches have been unable to produce $In(OH)_3$ nanotubes or their heterostructural derivatives or analogues.

An SEM image of the as-collected product is shown in Figure 1 A. Numerous rod-like nanostructures are formed in high yield (>80%), most of which are straight and have diameters of 70–250 nm and lengths of 2–5 μm. The XRD pattern in Figure 1 B provides clear evidence that the product nanostructures are composed of two crystalline phases, namely body-centered cubic (bcc) $In(OH)_3$ (JCPDS: 85-1338; $a = 7.979$ Å) and tetragonal Sn (JCPDS: 86-2265; $a = 5.831$ and $c = 3.181$ Å). Several characteristic peaks from impurities of tetragonal SnO_2 are also detected in the XRD pattern, probably because of oxidation of Sn outside the nanotubes.

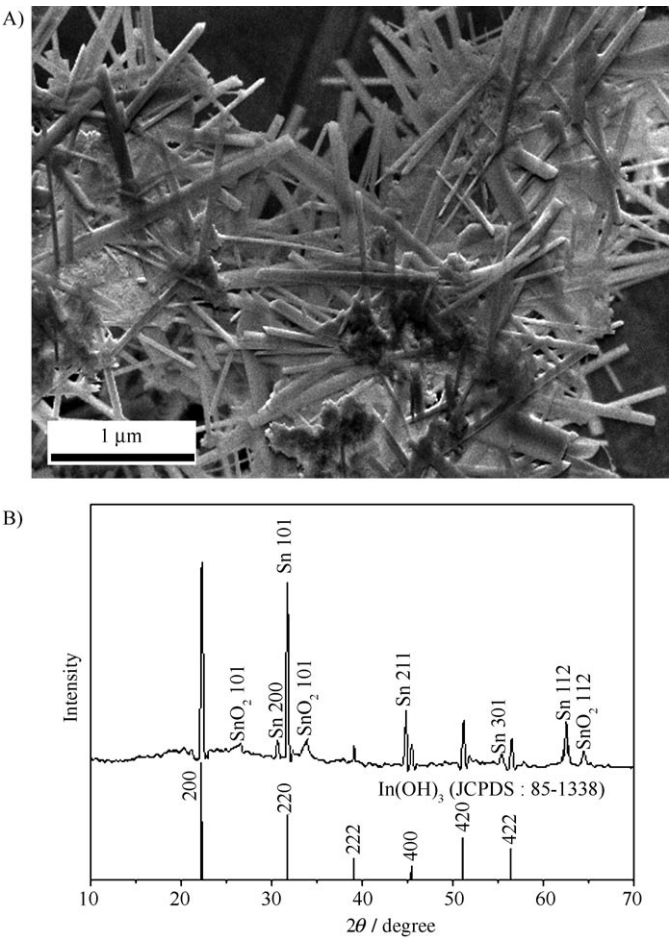

Figure 1. A) SEM image and B) XRD pattern of the as-collected product.

Figure 2 reveals more details about the nanostructures of the products, which are primarily Sn-filled $In(OH)_3$ nanotubes (Figure 2 A) along with a few empty $In(OH)_3$ nanotubes (Figure 2 B). The cross-sections of the nanotubes appear faceted (inset of B), and most filled nanotubes have uniform diameters and wall thicknesses throughout their whole

[*] Dr. Y. Fang, X. Wen, Prof. Dr. S. Yang
Department of Chemistry
The Hong Kong University of Science and Technology
Clear Water Bay, Kowloon, Hong Kong (China)
Fax: (+852) 2358-1594
E-mail: chsyang@ust.hk

[**] We are grateful to the Hong Kong University of Science and Technology for financial support under the grant HIA05/06.SC02. S.Y. also wishes to thank the Hong Kong Young Scholar Cooperation Research Foundation of NSFC.

Supporting Information for this article is available on the WWW under http://www.angewandte.org or from the author.

© 2006 Wiley-VCH Verlag GmbH & Co. KGaA, Weinheim

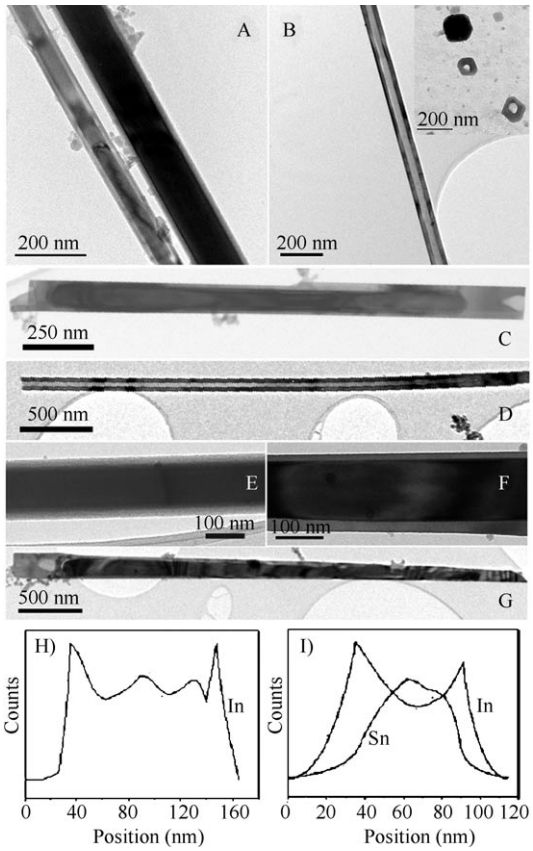

Figure 2. TEM characterizations of empty and filled nanotubes: A) two filled nanotubes; B) an empty nanotube and cross-sections of nanotubes (inset); C) a nanotube with two ends closed; D) a nanotube with one end open; E) a filled nanotube with walls of equal thickness; F) a filled nanotube with walls of unequal thickness; G) a filled nanotube whose diameter gradually decreases along the tube length; H) and I) line-scan EDS elemental profiles recorded for an empty nanotube and for a filled nanotube, respectively.

lengths (Figure 2A). It is interesting to note that the filled nanotubes are more abundant (about 80%) and always have their two ends closed (Figure 2C), whereas the empty nanotubes account for only around 20% of the tubes and have at least one of the ends open (Figure 2D). The TEM images show both symmetrical (Figure 2E) and lopsided (Figure 2F) thicknesses of the two side-walls of the filled nanotubes. This is consistent with the fact that the $In(OH)_3$ nanotubes are faceted and thus not cylindrically symmetric. A handful of filled nanotubes whose diameters and wall thicknesses gradually decrease along their lengths, for example from about 220 and 50 nm at the thicker end to about 80 and 20 nm at the thinner end (Figure 2G), are also observed. X-ray energy-dispersive spectroscopy (EDS) of the empty nanotubes gives an elemental ratio of In to O of about 1:3, whereas that of the filled nanotubes contain Sn as well as In and O (In:O:Sn $\approx$ 19:57:24). The empty nanotubes are made up of $In(OH)_3$, whereas the filled nanotubes consist of walls of $In(OH)_3$ and interiors filled with Sn. This was corroborated by line-scan EDS elemental profiles. One example is for an empty $In(OH)_3$ nanotube with a diameter of 140 nm and a wall thickness of about 30 nm (Figure 2H), and the other is for an $In(OH)_3$ shell about 10–20 nm thick with a filling of Sn about 70 nm across (Figure 2I).

The nanotube structures were further examined by recording high-resolution TEM images and electron diffraction patterns, as shown in Figure 3. One can immediately see

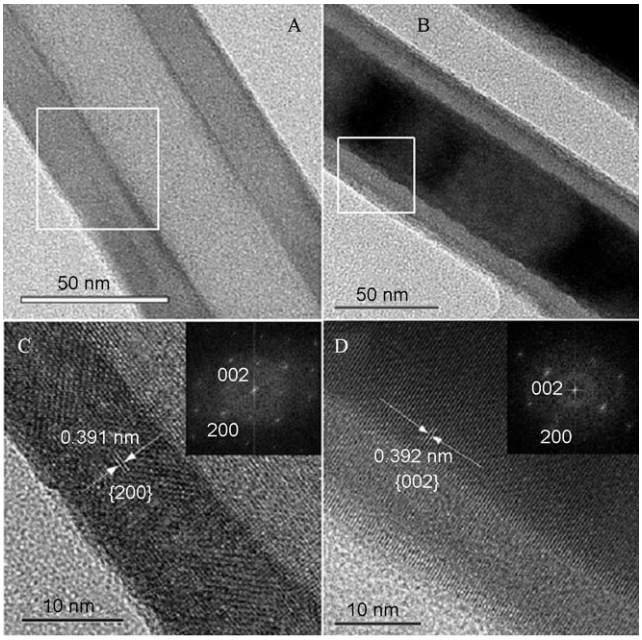

Figure 3. HRTEM images and the corresponding FFT patterns (insets) of an empty $In(OH)_3$ nanotube (A and C) and a Sn-filled $In(OH)_3$ nanotube (B and D). C and D are taken from the squares in A and B, respectively.

the uniform, well-defined single-crystalline structure of the $In(OH)_3$ nanotubes both without (Figure 3A) and with the Sn filling (Figure 3B). The HRTEM image in Figure 3C, taken for the area marked by a square in Figure 3A, shows clear lattice fringes for the (200) planes parallel to the tube axis, with a *d* spacing of 0.391 nm. The fast Fourier transform (FFT) pattern (inset in Figure 3C) can be indexed to bcc $In(OH)_3$ and the nanotubes grow along the *a*, *b*, or *c* axes of the $In(OH)_3$ crystal. A similar HRTEM image, taken from the area highlighted by the square in Figure 3B, is given in Figure 3D for a Sn-filled $In(OH)_3$ nanotube. Clear fringes perpendicular to the nanotube axis can be seen here as well. These fringes have an interplanar spacing of 0.392 nm, in accordance with the distance between the (002) crystal planes of $In(OH)_3$, which suggests the same growth direction as for the empty nanotubes. This observation is also mirrored in the FFT pattern (inset of Figure 3D) of this HRTEM image.

During TEM observations, we found that electron-beam irradiation in the microscope could induce fluidic movement of the Sn filling in the $In(OH)_3$ nanotubes. Figure 4 shows consecutive TEM images recorded during electron-beam irradiation of the imaged portion of the nanotube. Upward movement of the molten Sn core (by about 60 nm) inside the nanotube is vividly portrayed as a wavy form, which means that the Sn filling undergoes a melting phase transition upon electron-beam irradiation. It appears that part of the driving

 © 2006 Wiley-VCH Verlag GmbH & Co. KGaA, Weinheim

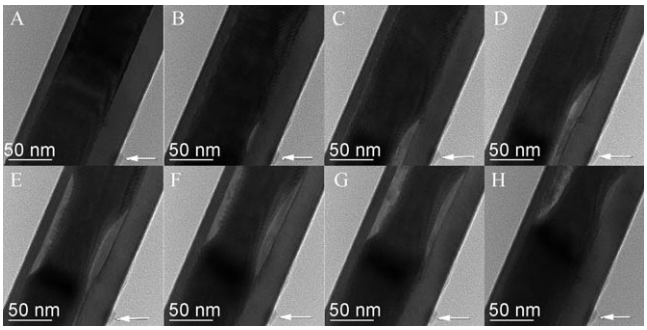

Figure 4. Consecutive TEM images (A to H) taken during electron-beam irradiation of the imaged portion of the nanotube. The arrows point to the same overhanging feature of the nanotube and indicate that the molten Sn moves upward.

force for the movement of the molten Sn core is its thermal expansion and non-wetting contact with the $In(OH)_3$ nanotube at the low base pressure of the TEM chamber. With better control, this effect could be developed into a nanoscale thermometer. A similar phenomenon has been observed previously for nanotube-encapsulated metals under electron-beam irradiation.[10] A significant melting point depression has also been observed for Ge semiconductor nanowires confined in carbon nanotubes, which could be the case for our Sn-filled $In(OH)_3$ nanotubes as well.[11] It is envisaged that the electron irradiation method may be a useful tool for tailoring the metal filling inside the nanotubes. For example, one could divide the metallic core into uniform nanoparticles to form a 1D array with controlled inter-particle spacings.

In order to shed light on the growth mechanism of the heterostructured $Sn@In(OH)_3$ nanowires, we resort to the binary phase-diagram of In and Sn shown in Figure 5A. Since the melting points, T, of In and Sn are 156.6 and 231.86 °C, respectively, Sn is expected to dissolve slowly in the molten In to form In–Sn liquid droplets (Figure 5A) at 180 °C with less than 65% Sn (point X), above which solid Sn starts to precipitate [see Eq. (1)].

$$\mathrm{In\,(liquid) + Sn\,(solid) \rightarrow In-Sn\,(liquid)} \quad (1)$$

As the reduction potential of In is more negative (ca. −1.00 V) than that of Sn (ca. −0.91 V) in weakly basic solution,[12] In is preferentially oxidized to $Sn@In(OH)_3$ (solid) in the form of a core–shell nanostructure by the oxygen in solution [Eq. (2)].

$$\mathrm{In-Sn\,(liquid) + O_2 + H_2O\,(solution) \rightarrow Sn@In(OH)_3\,(solid)} \quad (2)$$

A critical step in the nanotube formation is the initial elongation. This is achieved by the right combination of materials. Specifically, the nucleation of solid $In(OH)_3$ is accompanied by the deposition of solid Sn, both of which are necessarily in contact with the In–Sn droplet during growth so as to ensure a lowest energy path. This is only possible in a tube geometry, as illustrated in Figure 5B. Note that the reaction/deposition takes place on the surface of the In–Sn droplet to form an $In(OH)_3$ shell surrounding a solid Sn rod. After the liquid droplet has been consumed, assembly of the

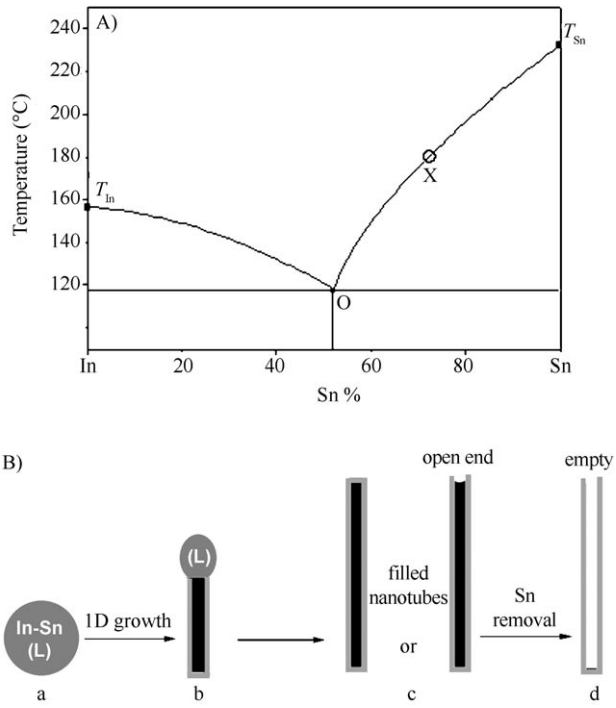

Figure 5. A) Binary phase diagram of In–Sn. B) Illustration of the growth process of Sn-filled $In(OH)_3$ nanotubes and the formation of empty $In(OH)_3$ nanotubes. The molten In reacts with solid Sn to form In–Sn liquid droplets (a). The reaction in Equation (2) then takes place on the surface of these liquid In–Sn droplets to form solid $In(OH)_3$, which is accompanied by the deposition of solid Sn. This leads to the elongation of a solid $Sn@In(OH)_3$ core/sheath nanostructure (b). Finally, continuous 1D growth consumes the liquid droplet, thereby completing the SLSS assembly of the $Sn@In(OH)_3$ core/sheath nanostructure (c). The empty $In(OH)_3$ nanotubes may be formed by dissolution of the Sn core of the $Sn@In(OH)_3$ nanotubes, which have at least one end open, in weakly basic aqueous ethanol solution (d).

Sn-filled $In(OH)_3$ nanotube is completed either with the top end closed or open depending on the availability of the necessary shell materials. Empty $In(OH)_3$ nanotubes may arise from dissolution of the Sn cores of the $Sn@In(OH)_3$ nanotubes with at least one end open in the weakly basic aqueous ethanol solution. This is in excellent agreement with the observation that the filled nanotubes always have their two ends closed, whereas the empty nanotubes have at least one of the ends open. We coin this unique 1D core–shell growth mode a solution–liquid–solid–solid (SLSS) process (see Figure 5B for details). This is an interesting extension of the SLS method with the difference of employing an alloy droplet and an additional solid deposition process to form the 1D core–shell nanostructure.

Control experiments have shown that the $Sn@In(OH)_3$ nanotubes can only be formed with the right combination of materials and reaction conditions. The aqueous ethanol solution provides the weakly basic environment necessary for the smooth precipitation of $In(OH)_3$, deposition of Sn, and the subsequent 1D growth guided by the In–Sn droplets. A solution that is either too acidic or too basic would be apt to dissolve the deposited $In(OH)_3$ shell, which would eventually

 © 2006 Wiley-VCH Verlag GmbH & Co. KGaA, Weinheim

halt the 1D growth (see Supporting Information). We also found that a solution of urea results in the formation of a dandelion-like architecture made up from a single layer of radially oriented $In(OH)_3$ nanorods surrounding a Sn core (see Supporting Information). We have therefore established some of the materials and environmental requirements for the 1D growth of the core–shell nanostructure.

To conclude, a one-step SLSS growth mode has been discovered that allows the first synthesis of empty single-crystalline $In(OH)_3$ nanotubes as well as nanotubes filled with Sn. The shells of the nanotubes have a cubic structure and grow along the *a*, *b*, or *c* axes of the $In(OH)_3$ crystal. It might be possible to convert the $In(OH)_3$ nanostructures into nanostructures of In_2O_3 which is a more common semiconductor, by annealing at elevated temperatures. The 1D SLSS growth mode is distinguished from the SLS method by the presence of an alloy droplet, on which reaction and deposition occur to form a solid shell and a solid core at the same time. A nanofluidic flow of the internal Sn has been observed when the environmental temperature is increased by electron-beam irradiation. This property could be exploited to engineer desired nanostructures inside the nanotubes. Our work suggests a new, general working mechanism for the growth of heterostructured core–shell nanowires by a simple solution procedure. With a judicious choice of alloy droplet and reaction and process conditions, one should be able to fabricate nanotubes with different compositions, sizes, morphologies, and heterostructures.

Experimental Section

The synthesis was carried out by lapping a piece of indium foil ($7 \times 7 \times 0.25\ mm^3$, 99.9%, Aldrich) with a piece of Sn foil ($10 \times 10 \times 0.25\ mm^3$, 99.9%, Aldrich) with a gentle press and placing the two at the bottom of a Teflon-lined stainless steel autoclave (25 mL) containing a solution of 0.5 M NaOH (0.5 mL), ethanol (10 mL), and distilled water (10 mL). The foils were carefully washed with ethanol before loading. The solution was heated to 180 °C and kept at this temperature for 30 h to give a gray powder and a chunk of incompletely reacted Sn foil. This was discarded and the gray powder was rinsed with ethanol and dried in air for characterizations. The structures were determined by powder X-ray diffraction (XRD, Philips PW-1830 X-ray diffractometer with $Cu_{K\alpha}$ irradiation, $\lambda = 1.5406$ Å, at a scan speed of $0.025\ deg\ s^{-1}$ over the 2θ range 10–70°). Morphologies were examined by scanning electron microscopy characterizations (SEM, JEOL 6300 and JEOL 6700F at an accelerating voltage of 15 kV). TEM observations were carried out with a JEOL 2010F microscope operating at an accelerating voltage of 200 kV. For both SEM and TEM characterizations the powder sample was dispersed in ethanol—the powder samples were embedded in epoxy resin and ultramicrotomed to obtain a cross-sectional view—and the suspension sonicated for 20 min. A drop of the suspension was then placed onto a silicon substrate or a copper grid coated with a holey carbon film and the solvent allowed to evaporate in air.

Received: March 15, 2006
Published online: June 22, 2006

Keywords: crystal growth · indium · nanotubes · semiconductors · tin

[1] a) L. J. Lauhon, M. S. Gudiksen, D. Wang, C. M. Lieber, *Nature* **2002**, *420*, 57; b) J. Q. Hu, Q. Li, X. M. Meng, C. S. Lee, S. T. Lee, *Chem. Mater.* **2003**, *15*, 305; c) W. Han, A. Zettl, *Adv. Mater.* **2002**, *14*, 1560; d) J. Hu, Y. Bando, Z. Liu, *Adv. Mater.* **2003**, *15*, 1000; e) Y. B. Li, Y. Bando, D. Golberg, *Adv. Mater.* **2003**, *15*, 581; f) Y. H. Gao, Y. Bando, *Nature* **2002**, *415*, 599.

[2] a) J. J. Wu, T. C. Wong, C. C. Yu, *Adv. Mater.* **2002**, *14*, 1643; b) K. K. Lew, L. Pan, E. C. Dickey, J. M. Redwing, *Adv. Mater.* **2003**, *15*, 2073.

[3] a) Y. Xie, P. Yan, J. Lu, Y. Qian, S. Zhang, *Chem. Commun.* **1999**, 1969; b) Y. G. Guo, L. J. Wan, C. L. Bai, *J. Phys. Chem. B* **2003**, *107*, 5441; c) J. Cao, J. Z. Sun, J. Hong, H. Y. Li, H. Z. Chen, M. Wang, *Adv. Mater.* **2004**, *16*, 84.

[4] a) A. M. Morales, C. M. Lieber, *Science* **1998**, *279*, 208; b) H. M. Lin, Y. L. Chen, J. Yang, Y. C. Liu, K. M. Yin, J. J. Kai, F. R. Chen, L. C. Chen, Y. F. Chen, C. C. Chen, *Nano Lett.* **2003**, *3*, 537; c) A. Kolmakov, Y. Zhang, M. Moskovits, *Nano Lett.* **2003**, *3*, 1125.

[5] a) T. J. Trentler, K. M. Hickman, S. C. Goel, A. M. Viano, P. C. Gibbons, W. E. Buhro, *Science* **1995**, *270*, 1791; b) H. Yu, W. E. Buhro, *Adv. Mater.* **2003**, *15*, 416; c) H. Yu, J. B. Li, R. A. Loomis, L. W. Wang, W. E. Buhro, *Nat. Mater.* **2003**, *2*, 517.

[6] a) D. C. Lee, F. V. Mikulec, B. A. Korgel, *J. Am. Chem. Soc.* **2004**, *126*, 4951; b) D. C. Lee, B. A. Korgel, *Mol. Simul.* **2005**, *31*, 637; c) J. D. Holmes, K. P. Johnston, R. C. Doty, B. A. Korgel, *Science* **2000**, *287*, 1471; d) T. Hanrath, B. A. Korgel, *J. Am. Chem. Soc.* **2002**, *124*, 1424; e) X. M. Lu, T. K. Hanrath, P. Johnston, B. A. Korgel, *Nano Lett.* **2003**, *3*, 93.

[7] T. Ishida, K. Kuwabara, *J. Ceram. Soc. Jpn.* **1998**, *106*, 381.

[8] S. Avivi, Y. Mastai, A. Gedanken, *Chem. Mater.* **2000**, *12*, 1229.

[9] a) H. L. Zhu, K. H. Yao, Y. H. Wo, N. Y. Wang, L. N. Wang, *Semicond. Sci. Technol.* **2004**, *19*, 1020; b) X. H. Zhang, S. Y. Xie, Z. M. Ni, X. Zhang, Z. Y. Jiang, Z. X. Xie, R. B. Huang, L. S. Zheng, *Inorg. Chem. Commun.* **2003**, *6*, 1445; c) D. B. Yu, S. H. Yu, S. Y. Zhang, J. Zuo, D. B. Wang, Y. T. Qian, *Adv. Funct. Mater.* **2003**, *13*, 497.

[10] a) W. K. Hsu, M. Terrones, H. Terrones, N. Grobert, A. I. Kirkland, J. P. Hare, K. Prassides, P. D. Townsend, H. W. Kroto, D. R. M. Walton, *Chem. Phys. Lett.* **1998**, *284*, 177; b) J. Q. Hu, Y. Bando, J. H. Zhan, D. Golberg, *Angew. Chem.* **2004**, *116*, 4706; *Angew. Chem. Int. Ed.* **2004**, *43*, 4606.

[11] Y. Y. Wu, P. D. Yang, *Adv. Mater.* **2003**, *15*, 520.

[12] a) *Inorganic Chemistry*, 3rd ed. (Eds.: X. Z. Cao, T. Y. Song, X. Q. Wang), Higher Education, Beijing, China, **2005**; b) *Lange's Handbook of Chemistry*, 15th ed. (Ed.: J. A. Dean), McGraw-Hill, New York, **1999**.

 © 2006 Wiley-VCH Verlag GmbH & Co. KGaA, Weinheim